
UNDERSTANDING INTRA-NODE COMMUNICATION IN HPC SYSTEMS AND DATACENTERS

Joaquin Tarraga-Moreno, Jesus Escudero-Sahuquillo, Pedro Javier Garcia, Francisco J. Quiles

Department of Computing Systems, Universidad de Castilla-La Mancha
Spain

antonioj.tarraga@uclm.es

March 3, 2025

ABSTRACT

Over the past decade, specialized computing and storage devices, such as GPUs, TPUs, and high-speed storage, have been increasingly integrated into server nodes within Supercomputers and Data Centers. The advent of high-bandwidth memory (HBM) has facilitated a more compact design for these components, enabling multiple units to be interconnected within a single server node through intra-node networks like PCIe, NVLink, or Ethernet. These networks allow for scaling up the number of dedicated computing and storage devices per node. Additionally, inter-node networks link these devices across thousands of server nodes in large-scale computing systems. However, as communication demands among accelerators grow—especially in workloads like generative AI—both intra- and inter-node networks risk becoming critical bottlenecks. Although modern intra-node network architectures attempt to mitigate this issue by boosting bandwidth, we demonstrate in this paper that such an approach can inadvertently degrade inter-node communication. This occurs when high-bandwidth intra-node traffic interferes with incoming traffic from external nodes, leading to congestion. To evaluate this phenomenon, we analyze the communication behavior of realistic traffic patterns commonly found in generative AI applications. Using OMNeT++, we developed a general simulation model that captures both intra- and inter-node network interactions. Through extensive simulations, our findings reveal that increasing intra-node bandwidth and the number of accelerators per node can actually hinder overall inter-node communication performance rather than improve it.

Keywords High-performance interconnection networks · Intra-node communication · accelerators · GPUs

1 Motivation

Supercomputers and Data centers are increasing their computing power and storage capacity to cope with the growing requirements of applications and services, such as those used in scientific computing or generative AI. While computing power requirements are currently being met using more powerful processors and specific-purpose accelerators (GPUs, TPUs, etc.), innovative technologies, such as 3D-stacked high-bandwidth memory (HBM), Non-Volatile Memory (NVMe) or Storage Class Memory (SCM), are increasing storage and memory capacity and bandwidth access, to bring unprecedented amounts of data close to where it is processed and reduce inter-node communication latency.

The devices mentioned above (i.e., accelerators, CPUs, memory, or storage) are interconnected within end nodes through an intra-node interconnection network (also known as I/O or system interconnect), which must be designed so that it does not become the bottleneck in the communication among these devices. Generally, this is achieved by over-dimensioning the aggregated bandwidth of the intra-node network links. For instance, the Peripheral Component Interconnect Express (PCIe) is the *de-facto* intra-node network in contemporary servers, offering 1GB/s per lane for PCIe 3.0, 2GB/s for PCIe 4.0, and 4GB/s for PCIe 5.0. Other intra-node technologies exist such as NVLink (NVIDIA), which is specially designed to interconnect multiple GPUs at either the same end-node or different end-nodes, reaching speeds of 4GB/s, 7.5GB/s, and 15.1 GB/s per lane for Gen5, Gen6, and Gen7 (planned for next year), respectively.

Infinity Fabric (AMD) is also used to interconnect specific AMD devices for both CPU (i.e., Zen) and graphics (e.g., Vega). Therefore, the increasing link speed in the intra-node network and the variety of devices within a server node (i.e., CPUs, GPUs, TPUs, other accelerators, SSDs, NVMe, etc.) challenges the design of intra-node network technologies, which needs to thoroughly identify potential bottlenecks when different communication patterns are generated involving multiple end-node devices that request to communicate through the intra-node network at full speed.

In this context, communication operations among end-node devices (e.g., GPUs and other accelerators) may involve devices beyond a single node. For instance, an *AllReduce* communication operation performed when training a deep neural network (DNN) usually involves multiple GPUs that can be placed at different end nodes when the model to train does not fit a single end node [1]. Following this example, when the model is too big to be stored in the memory of a single end-node device, it is usually stored in the local memory of multiple end-node devices (e.g., the HBM local memory of GPUs). So, when the weights of that model need to be updated in a distributed manner, communication operations are generated involving multiple end-node devices, which will encapsulate the communication operations information in intra-node network transactions that will be exchanged among the devices involved in the communication, which may be placed at different end-nodes. More precisely, a communication operation involving two end-node devices (e.g., GPUs) can be divided into three phases. First, an end-node device generates an intra-node network transaction with the specific information to be transmitted. This transaction is divided into intra-node network packets and sent throughout the intra-node network to another device within the same end node or the network interface (NIC). In any of these cases, the receiving end-node device finally composes the transaction based on the received packets. Secondly, when the transaction is sent to a remote end-node device from the mentioned NIC, the intra-node transaction is encapsulated into inter-node network packets and sent through the inter-node network to the NIC at the destination end node. Third, at the NIC at the receiving end-node, packets are combined into an intra-node network transaction, divided into intra-node packets, and sent through the intra-node network reaching the destination end-node device, which finally processes that transaction. Note that the interconnection network performance has been widely studied in the last decades only assuming the second communication phase. However, the impact of communication phases first and second in the intra- and inter-node network performance is still a wide-open field of study [2]. Therefore, it is critical to accurately analyze the communication operations generated at end-node devices under specific communication patterns and their impact on the intra- and inter-node network performance. This analysis will help identify potential communication bottlenecks in the system.

Note that the aggregated communication bandwidth that multiple end-node devices may require at a given instant can also be requested to the inter-node interconnection network when devices at different end nodes want to communicate. Consequently, the inter-node network bandwidth is augmenting proportionally to accommodate the communication requirements of the increasing number of devices per end node and their computing power and storage requirements. Furthermore, current inter-node interconnection network technologies are focused on proposing more cost-effective network topologies, routing algorithms, and specific mechanisms to improve network performance in several ways, such as congestion control, power management, QoS, network virtualization, fault tolerance, etc.

This paper addresses the following research question: *to what extent does the intra-node network communication impact the inter-node communication and vice-versa?* To answer this question, we have characterized the intra-node network architecture and the communication operations (intra- and inter-node) generated at end-node devices and modeled them into an OMNeT++-based simulation tool. Note that there are several proposals for system-level simulators (e.g., *gem5* [3]), which model accurately the processor, memory, GPUs, and I/O. Other solutions model the specific GPU-to-GPU communication (e.g., *TraceR-CODES* [4, 5]). However, these models lack scalability or an accurate performance model at the packet level for the combined intra-node and inter-node communication. We have validated our simulation model using a real cluster infrastructure. We have run specific micro-benchmarks (e.g., InfiniBand Perftest and OSU benchmarks) and obtained latency and throughput metrics, which we have compared to those obtained using our simulation model. Moreover, we have performed simulation experiments configuring intra- and inter-node networks that communicate 32 and 128 end-nodes (and 256 and 1024 accelerators, respectively) using realistic communication patterns, such as those used in the training of Large Language Models (LLMs) for generative AI. The obtained results show that the intra-node network can be a bottleneck, due to the interference between intra-node and inter-node communication operations, increasing dramatically the tail latency at high intra- or inter-node traffic loads.

The rest of the paper is organized as follows. Section 2 overviews the background of end-node devices, inter- and intra-node interconnects, and communication patterns. Section 3 describes our proposed simulation model to analyze the impact of intra- and inter-node communication interference. Section 4 describes the simulation experiments and discusses the obtained results. Finally, Section 5 draws some conclusions.

2 Background

This section provides background details on end-node devices and the interconnection network architecture. Moreover, we analyze critical communication patterns from typical applications currently run in supercomputers and data centers.

2.1 End-node devices

The Central Processing Unit (CPU) is the central component at server nodes in supercomputers or data centers. The CPU manages all processes and jobs within the node and interprets and executes instructions to coordinate software and hardware operations. For instance, in generative AI applications based on Large Language Models (LLMs), the CPU prepares and preprocesses vast datasets before sharing them to GPUs or TPUs for training.

The Graphics Processing Unit (GPU) is a specialized processor optimized for computations requiring massive parallelism. Unlike CPUs, which excel in sequential task execution, GPUs feature thousands of smaller cores designed for simultaneous operations. This architecture makes GPUs critical for the training and inference in LLMs. Leading manufacturers such as NVIDIA, AMD, and Intel have developed GPUs tailored for intensive AI workloads. For instance, the NVIDIA Hopper GPU [6] is one of the most advanced GPUs of this company. It combines high memory bandwidth (HBM), increased computational power, and seamless communication via the specific NVLink intra-node network. The NVIDIA Hopper GPU is integrated into the Grace Hopper Superchip [7], which combines the NVIDIA Hopper GPU with the NVIDIA Grace CPU. It delivers up to 989.4 TFLOPS in FP32 and features up to 144GB of HBM3e memory, making it a famous solution for AI training and inference. Alternatively, the Intel Gaudi GPU [8] is a powerful GPU designed for large-scale AI training and inference. It provides support for massive datasets and seamless integration into various systems. Intel Gaudi GPUs deliver up to 229 TFLOPS with 128GB of HBM memory, making it a serious contender in the AI hardware market.

Solid State Drives (SSDs) and other high-speed storage technologies (e.g., NVMe or SCM) are also key components in data centers and supercomputers. They provide the necessary storage capacity and data retrieval speeds to support the large datasets typical of generative AI and HPC workloads. The performance of memory disks directly impacts data transfer rates, latency, and overall system efficiency. Emerging technologies, such as NVMe over Fabrics (NVMe-oF) enhance storage performance, bridging the gap between compute and data requirements in large-scale systems.

The end-node devices mentioned above are interconnected using an intra-node network. They can also communicate with other devices placed at different end nodes using an inter-node network. The network interface (NIC) processes intra-node packets and injects them into the inter-node network.

2.2 Inter-node interconnection networks

They are a critical subsystem in Supercomputers and Datacenters to provide high-performance communication operations among thousands of end nodes at a reduced cost; reliability, since large-scale interconnection networks increase fault probability; and energy efficiency to minimize the network energy fraction.

In the past, inter-node networks for Supercomputers and Data centers have differed in multiple ways. Nonetheless, in recent years, the architecture of these networks in these two different systems has converged [9] thanks to standard communication requirements of the applications run in these systems. However, the trend nowadays is designing high-performance inter-node networks interchangeable between Supercomputers and Datacenters. Indeed, inter-node interconnection networks for these systems share critical network design aspects, such as the topology, routing algorithm, flow control, quality of service (QoS), power management, and congestion control. Although the research and innovations in these networks have been pervasive during the last decades to overcome these design aspects, the post-Exascale era and Generative AI models pose new challenges to the interconnection network design [10].

Numerous manufacturers provide fast and efficient network technologies, such as NVIDIA and its InfiniBand-based network devices, HPE and Cray, which promote the Slingshot technology, or all the partners composing the recently created Ultra Ethernet Consortium (UEC), whose primary goal is to optimize the Ethernet network technology for high-performance AI and HPC. For instance, the RDMA over Converged Ethernet (RoCE) is an advanced protocol implemented in NVIDIA devices that enables Remote Direct Memory Access (RDMA) over Ethernet networks. RoCE is designed to reduce CPU overhead, lower latency, and improve throughput by bypassing traditional TCP/IP stacks. It is widely used in inter-node communication within Datacenters, especially for storage and high-performance computing (HPC). An interesting implementation of RoCE can be found in Intel's Gaudi3 system, which leverages RoCE to optimize the performance of AI training workloads. By integrating RDMA capabilities directly into the system architecture, Gaudi3 achieves efficient inter-node communication while minimizing latency and maximizing data throughput.

The different inter-node network technologies mentioned above share common design goals. For instance, regarding link speed, they feature new signaling methods, form factors, and single- and multi-mode fiber at speeds of 200, 400, and 800 Gbps, which are growing exponentially, so that it is expected they will reach Terabit speed (TbE technology) within this decade.

2.3 Intra-node interconnection networks

They are also a fundamental subsystem at end nodes of Supercomputers and Data centers. Intra-node networks must offer ultra-low latency to facilitate communication between CPUs, accelerators, and memory; high bandwidth to support data-intensive workloads; and energy efficiency to ensure sustainable performance. Furthermore, as end nodes become increasingly heterogeneous due to the combination of CPUs, GPUs, and specialized accelerators, the intra-node networks cope with new communication patterns. Historically, these patterns have been simple, so the intra-node networks were based on bus-based or ring-based interconnects. However, modern intra-node networks have evolved significantly to accommodate the demand for higher performance and scalability. Nowadays, intra-node networks support emerging workloads, such as generative AI models that demand unprecedented levels of parallelism and data movement efficiency [11]. Consequently, intra-node interconnection networks incorporate innovations such as in-network hardware accelerators for specific communication patterns, advanced routing algorithms, novel flow control techniques, power-aware communication strategies, etc.

PCIe is the mainstream interconnect between CPUs, GPUs, network cards, and storage devices. The PCIe bandwidth and low latency enable efficient data transfers crucial for modern high-performance workloads. PCIe speeds have evolved significantly, with PCIe 5.0 and PCIe 6.0 offering per-lane speeds of up to 3.9 and 7.5 GB/s, respectively. These advancements improve the throughput and reduce communication bottlenecks. PCIe is used, for instance, to scale up the Intel's HL-325L Habana Gaudi 3 accelerators within a single node. Furthermore, PCIe is a foundational interconnect for inter-node network interface cards (NICs), directly impacting the overall system performance by reducing data movement delays and enhancing throughput. By contrast, NVLink (NVIDIA) provides significantly higher bandwidth than PCIe, with the latest versions supporting up to 900 GB/s of bidirectional bandwidth. This capability enables seamless data sharing between GPUs, CPUs, and memory subsystems, making it particularly effective for AI/ML workloads and other compute-intensive applications. NVLink is also employed in certain inter-node contexts, such as NVIDIA DGX systems, where it enhances the scalability and performance of multi-node configurations by creating tightly coupled GPU clusters.

There are other intra-node network solutions, such as Infinity Fabric (AMD) or Quick Path Interconnect (Intel), and even open-standard efforts such as the UALink Consortium that are also playing an important role in the intra-node networks design. Furthermore, emerging standards and protocols, such as the Compute Express Link (CXL), aim to unify memory and compute interconnects, enhancing intra-node communication efficiency.

2.4 Communication Patterns

The communication operations generated by emerging applications may threaten the performance of intra- and inter-node interconnection networks. With the rapid growth of generative AI applications, dominated by Large Language Models (LLMs), the size of these models are expanding so they no longer fit on a single GPU or even in the GPUs of a single end node. Therefore, parallelization is needed to accelerate LLM training and inference. The parallel programming model used to leverage the computing power and storage capacity of these systems is currently based on two main types of parallelism: data parallelism and model parallelism.

On the one hand, *Data Parallelism* (DP) [12] distributes the training process across multiple computational devices by dividing the dataset into smaller chunks (or batches). Each device (or group of devices) processes its assigned data portion independently, using an identical model copy. DP enables efficient scaling and faster processing. During training, communication between model copies occurs after a batch is processed when gradients are computed and updated. At this stage, each model copy exchanges gradient updates with all other copies using an *AllReduce* communication operation. This communication step ensures consistent parameter updates across all model replicas.

By contrast, *Model Parallelism* (MP) distributes large-scale models across multiple computational devices, when these models do not fit in a single device. For instance, LLMs, such as GPT-3, GPT-4, and PaLM, have billions of parameters, making them too large to fit into the memory of a single accelerator. Several approaches exist to MP, such as Tensor Parallelism [13] and Pipeline Parallelism [14]. Specifically, *Tensor Parallelism* (TP) divides individual operations (e.g., matrix multiplications or tensor computations) across multiple devices. Each device performs a portion of the computation, working on tensor subsets. In the training phase, communication is required during the execution of these operations, as the intermediate results need to be shared between devices. Forward and backward passes involve frequent communication to synchronize gradients, typically using an *AllReduce* or *AllGather* operation for each gradient

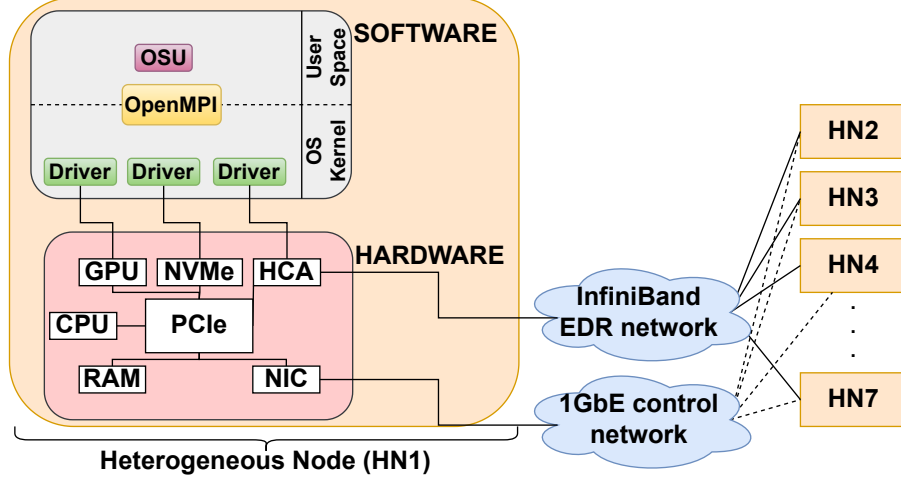


Figure 1: Node configuration in the CELLIA cluster.

update. Due to the high communication frequency and the need for low latency and high throughput, tensor parallelism is most effective when implemented within a single computing node. By contrast, *Pipeline Parallelism* (PP) splits the model into stages, such as groups of layers, assigning each stage to a separate device. Data flow sequentially through these stages, enabling pipelined execution where different input computations overlap. Communication occurs when intermediate activations or gradients are passed between stages (i.e., accelerators) during forward and backward propagation. Unlike TP, PP involves point-to-point communication between devices at stage boundaries. While PP benefits from low-latency communication, its lower communication intensity makes it feasible to implement across multiple end nodes.

3 Intra- and inter-node simulation model

This section describes the intra- and inter-node interconnection network simulation model that we have developed to study the impact of intra-node communication on the performance of the intra- and inter-node interconnection network. We also describe the characterization of realistic communication patterns as those generated by emerging applications, such as LLMs. In the following sections, we describe the server node architecture that has inspired the generic simulation model, the characterization of the PCIe communication on that server node, the proposed generic intra- and inter-node simulation model, and the network traffic model that mimics the behavior of realistic communication operations in LLM parallel training.

3.1 Baseline end-node architecture

Since we want to validate the simulation model against a real infrastructure before performing scale-out simulations, we have used an end-node architecture based on PCIe 3.0 as the baseline for our simulation model. Figure 1 illustrates the architecture of an end node in the *Cluster for the Evaluation of Low-Latency Architectures* (CELLIA).

The CELLIA cluster comprises several computing nodes with GPUs and NVMe disks. Specifically, each one of these end nodes has two CPUs, Intel Xeon Silver 4116, connected to the PCIe Gen3, and 192GB of RAM. These nodes also have an EDR InfiniBand network interface (a.k.a. HCA) MCX556A-ECAT ConnectX-5 dual-port. The InfiniBand EDR technology provides a data rate of 100 Gbps per HCA port (i.e., 12.5 GB/s), with packets of 4 KiB of MTU. These packets contain a 64B header and a 4032B payload. This cluster has a management 1GbE network, so each node has a network interface (NIC) for management purposes. In addition, each node has installed an NVIDIA Tesla T4 GPU over PCIe Gen3 x16 and an NVMe disk Ultrastar SN200 Series NVMe SSD over PCIe Gen3 x8. This versatility allows the node to perform a wide range of tasks, and we aim to model each component comprehensively to simulate various scenarios effectively.

Note that this heterogeneous node architecture has several devices attached to the PCIe (e.g., the CPU, GPU, NVMe, and HCA), so the intra-node network could be a bottleneck when inter-node communication involves other devices placed in different nodes. In the following section, we describe the characterization of the communication involving the intra-node network based on PCIe and the inter-node network.

3.2 PCIe communication characterization

To accurately model the PCIe subsystem communication, we first need to understand the specific characteristics of the PCI-Express system. We assume PCI-Express version 3.0, which can transfer data at 8 Gbps per lane. Since our HCA¹ transmits over 16 PCI lanes, the total data transfer rate from the intra-node network to the HCA can reach up to 128 Gbps (i.e., 16GB/s). Considering the PCIe version and its 128b/130b encoding, we can transfer accurate data close to 126 Gbps. At the same time, the HCA can inject traffic into the inter-node network at a maximum rate of 100Gbps since it is InfiniBand EDR technology. Thus, the intra-node communication may become a bottleneck when the HCA is saturated. Figure 2 shows the number of PCIe lanes and maximum payload size (MPS) for the different end-node devices. We assume that our PCIe communication model adjusts the MPS to 128B.

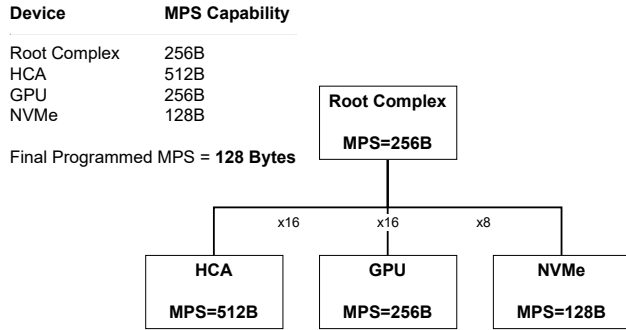


Figure 2: PCIe cluster maximum payload size (MPS).

We assume that all end-node devices are connected through a PCIe Root Complex (RC) without using PCIe switches (see Figure 1). This PCIe configuration can impact communication performance between two different endpoints (E1 and E2), as the communication model follows the following steps: $EP1 \rightarrow RC \rightarrow CPU \rightarrow RC \rightarrow EP2$. As end nodes in our real cluster follow this approach, and we want to validate our simulation model compared to these nodes, we have modeled this PCIe communication. Note that the CPU and RC involvement in the communication impact performance, especially when communicating between two end-node devices that do not require CPU involvement. The most efficient path typically uses a PCIe Switch, through which these devices communicate directly. By contrast, the CPU can communicate with the HCA in our tests by traversing the RC only once.

Our intra-node baseline model is focused on PCIe Gen3 parameters, including its data rate, *AckFactor*, and encoding. These parameters determine the time required to process each PCIe message in our system. The PCIe Gen3 communication time is determined by the processing time taken by the end-node devices to compute each packet composition and decomposition, and the time taken to process and transmit each PCIe packet (Transaction Layer Packets or TLPs and Data Link Layer Packets or DLLPs). The resulting intra-node latency for each message in a PCIe communication is expressed in the following set of equations:

¹We use the term *Host Channel Adapter* (HCA) from the InfiniBand jargon to distinguish it from the 1GbE NIC in our assumed end-node model.

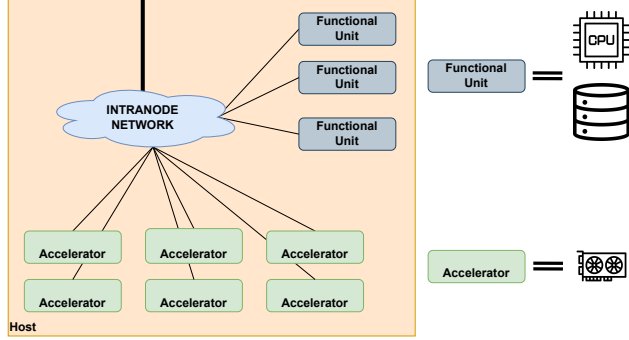


Figure 3: SAURON simulator host architecture.

$$\begin{aligned}
 BytesPerNs &= \frac{Width}{\frac{1}{DataRate \times Encoding}} \\
 TLPTime &= \frac{TLPOverhead + MaxPayloadSize}{BytesPerNs} \\
 DLLPTime &= \frac{DLLPOverhead + DLLPSize}{BytesPerNs} \\
 NumberTLPs &= \frac{MessageSize}{MaxPayloadSize} \\
 NumberACKs &= \frac{NumberTLPs}{AckFactor} \\
 LatencyTime &= NumberTLPs \times TLPTime + \\
 &\quad NumberACKs \times DLLPTime
 \end{aligned} \tag{1}$$

Where $BytesPerNs$ is the number of bytes that a PCIe link can transmit per nanosecond (ns), determined by $Width$ that indicates the number of lanes of the link, $DataRate$ that indicates the transmission rate determined by the PCIe version, and $Encoding$ that express the number of bits of data that are encoded in each transmission, also determined by the PCIe version. Next, the $TLPTime$ represents the time required to transmit a TLP over a PCIe link, given by the $TLPOverhead$ that is the overhead introduced in each TLP, the $MaxPayloadSize$ that is the maximum data contained in each TLP, and the $BytesPerNs$ value. The $DLLPTime$ is the time required to transmit a DLLP over a PCIe link, which is given by $DLLPOverhead$ and $DLLPSize$ that represent the overhead and data in each DLLP, and $BytesPerNs$. We also need to compute the $NumberTLPs$, which is the number of TLPs in which it is split each message to be sent over the intra-node network, determined by the message size ($MessageSize$) and the MPS ($MaxPayloadSize$). The $NumberACKs$ is the number of ACKs to send over the intra-node network, determined by dividing $NumberTLPs$ by $AckFactor$, which is the maximum number of TLPs that can be received before sending an ACK message. Finally, the $LatencyTime$ of our communication model sums the time it takes to send all TLPs and ACKs.

This communication model allows us to reproduce the PCIe transactions with a high level of detail. As described in section 4.1, we have validated this model compared with the communication operations generated in a real cluster.

3.3 Generic intra-node network model

Apart from incorporating the PCIe model described before, we have extended the SAURON network simulator [15]. to model a generic intra-node network and realistic communication patterns. SIM is a highly scalable simulator that models various inter-node communication patterns, topologies, and intra- and inter-node network configurations. Figure 3 shows the end-node generic architecture modeled in the SIM simulator.

We assume a configurable number of accelerators and other functional units (e.g., CPUs or storage devices) interconnected “all-to-all” using a switch in the intra-node interconnection network. This switch can be configured to provide the desired bandwidth so the intra-node network can process the incoming traffic addressed to the end-node devices, and the outgoing traffic they generate. Indeed, we can also configure the bandwidth between this switch and the end-node NIC, i.e., the bandwidth between the intra- and inter-node network. Note that this generic model permits configuring the intra-node network according to emerging technologies (e.g., PCIe Gen4, Gen5, Gen6, NVLink, Habana Gaudi, etc.). Indeed, we can configure the number of lanes, the bandwidth for the different end-node devices, their maximum payload size (MPS), etc.

We assume messages are generated at accelerators (GPUs, TPUs, etc.) and functional units (CPUs, NVMe, etc.). Messages at these devices are split into packets (according to the intra-node network MPS) and injected into the intra-node network. Note that these packets can be addressed to other devices in the same or different end nodes. In the latter case, NICs convert the intra-node packets to inter-node packets and inject them into the inter-node network. This conversion involves populating inter-node packets, with a size (i.e., MTU) different from that of intra-node packets, with the header and payloads of inter-node network packets. Therefore, this conversion may introduce additional latency.

As described in the following section, we can configure the message size at accelerators and functional units, the destination distribution, and the generation rate in our model. This flexibility permits reproducing the communication patterns observed in the training phase of LLMs when several types of parallelism are used (e.g., DP, TP, or PP).

3.4 Generic LLM communication modeling

We have modeled network traffic generated by LLMs, specifically during the training phase. To accurately capture LLM communication traffic characteristics, we have considered different approaches. First, AI training follows a cyclic pattern, where communication operations repeat across data batches provided to the LLM. In this context, it is essential to distinguish between Data Parallelism (DP) and Model Parallelism (MP), as described in Section 2.4. Between these communication operations, accelerators (e.g., GPUs) perform computation tasks until reaching different sub-layers (e.g., Multi-Head Attention (MHA), Feed-forward Neural Network (FFN)), which then trigger new communication operations. In our case, all accelerators have identical computational capabilities, processing the same amount of data at the same speed. As a result, all accelerators initiate their next communication operation simultaneously.

We assume the LLM is already stored in the accelerators’ memory, eliminating the need to exchange messages with external memory resources (e.g., NVMe disks). Instead, all communication occurs between accelerators to share information during the Forward and Backward passes in MP or to update gradients in DP. Our LLM communication model defines five distinct traffic patterns: $C1$, $C2$, $C3$, $C4$, and $C5$. From $C1$ to $C4$, we model a massive LLM that requires MP to distribute the model across multiple accelerators. The key difference between these traffic patterns is the predominant form of MP: Tensor Parallelism (TP) or Pipeline Parallelism (PP).

$C1$ assumes that TP is used extensively, i.e., most sub-layer communications follow a TP pattern (e.g., AllReduce, AllGather operations). This scenario generates significant traffic due to the need to update gradients during forward and backward propagation between devices (see Section 2.4). As a result, this traffic pattern generates 20% of the communication to the inter-node network and 80% to the intra-node network. Next, $C2$ and $C3$ also employ MP; however, the transferred data size between devices is smaller as these configurations rely more on PP than TP. This reduces inter-node traffic, as PP primarily uses Point-to-Point operations. Specifically, these traffic patterns generate 15% and 10% of the traffic to the inter-node network, while 85% and 90% remain within the intra-node network, respectively. Finally, $C4$ uses MP without TP, relying exclusively on PP. In this case, inter-node communication is minimized (e.g., 5%), as fewer updates are required between stages. Consequently, intra-node network communication exceeds 95%.

By contrast, $C5$ does not implement MP. In this scenario, we assume the model is not large enough to require multiple accelerators. Since the model fits within a single accelerator, only DP is used to accelerate training, and no inter-node communication is needed. As a result, all communication occurs within the same node (100% intra-node communication).

4 Evaluation

This section describes the experiments conducted to validate our simulation model compared to a real cluster environment. We also show the results of scale-out simulations using realistic intra- and inter-node network configurations and communication patterns.

4.1 Simulation model validation

This section describes the validation of the PCIe intra-node simulation model compared to the baseline end-node architecture (see Section 3.1). We have performed two different experiments using the OSU micro-benchmarks [16] and the Infiniband performance tests [17] (IB Perfests). For the *OSU micro-benchmarks*, we used a host-based point-to-point latency test (`osu_latency`) that measures the latency between two compute nodes during a ping-pong message exchange of a certain data size. Many iterations of this exchange are executed and the average one-way latency value is obtained. As blocking `MPI_Send` and `MPI_Recv` functions are used, the waiting overhead at the host side is included in the latency values. To reduce this overhead, we used the *IB Perfests* that generate direct communication for user-space applications directly accessing the InfiniBand hardware, so they do not introduce the overhead of specific communication libraries. More precisely, we performed `ib_send_lat`, `ib_write_lat`, and `ib_read_lat` tests using payloads ranging from 128 Bytes to 4 MiB. As the MPS of the end-node PCIe hardware is 128 Bytes, messages smaller than this size have identical latency when they fit within a single 128B-payload TLP, so we omitted these values. Table 1 shows the bandwidth results for these tests when varying the generated message size.

Table 1: Bandwidth results (GiB/s) when communicating two nodes in the real cluster.

Msg. Size	osu_latency	ib_read	ib_write	ib_send
128 B	0.54	0.37	0.44	0.41
256 B	1.04	0.79	0.87	0.77
512 B	2.04	1.51	1.75	1.64
1 KiB	3.44	2.74	3.30	3.10
2 KiB	6.17	6.63	7.35	6.22
4 KiB	8.41	9.90	11.02	11.00
8 KiB	10.39	11.38	11.58	11.55
16 KiB	11.11	11.78	11.53	11.63
32 KiB	11.64	11.80	11.60	11.67
64 KiB	11.93	11.81	11.62	11.60
128 KiB	12.08	12.09	11.90	11.90
256 KiB	12.16	12.09	11.92	11.93
512 KiB	12.20	12.09	11.93	11.92
1 MiB	12.21	12.09	11.93	11.93
2 MiB	12.17	12.06	11.93	11.94
4 MiB	12.16	12.03	11.86	11.94

As we can see, the maximum link bandwidth for the `ib_read_lat` (i.e., around 12.1 out of 12.5 GB/s) is first achieved with 128KiB messages. Larger messages cannot reach a higher bandwidth due to the packet header overhead (i.e., 60B), since the maximum payload for 4KB MTU packets in the InfiniBand network is $4096 - 60 = 4036$. Anyway, the obtained link bandwidths are similar regardless whether OSU or IB Perfests are used.

Table 2 shows a similar trend in latency. OSU has higher latency than IB Perftest for intermediate message sizes, due to the blocking `MPI_Send` and `MPI_Receive` calls. As we have not included the host-side latency of specific communication libraries in the simulation model, we will focus hereafter on the IB Perftest tests.

Table 2: Latency results (in μ s) when communicating two nodes in the real cluster.

Msg. Size	osu_latency	ib_read	ib_write	ib_send
128 B	1.61	2.03	1.12	1.20
256 B	2.09	2.07	1.56	1.59
512 B	1.96	2.02	1.58	1.64
1 KiB	2.20	2.15	1.70	1.77
2 KiB	3.00	2.43	1.95	2.02
4 KiB	3.90	2.88	2.46	2.56
8 KiB	5.52	3.40	2.84	2.94
16 KiB	7.42	4.28	3.88	3.86
32 KiB	9.26	5.68	5.41	5.32
64 KiB	14.14	8.38	8.06	7.97
128 KiB	23.32	13.66	13.39	13.25
256 KiB	26.41	24.25	24.27	24.10
512 KiB	47.88	45.40	45.73	45.41
1 MiB	91.85	87.73	88.95	88.46
2 MiB	177.96	173.31	174.65	173.74
4 MiB	350.68	343.93	345.97	344.31

In sections 3.1 and 3.2, we described that the real cluster achieves speeds of over 12.5 GiB/s on the Infiniband inter-node network when transmitting raw data (i.e., without considering packet headers) and 16 GiB/s on the PCIe intra-node network. Therefore, the Infiniband network becomes the bottleneck when the intra-node network demands full speed

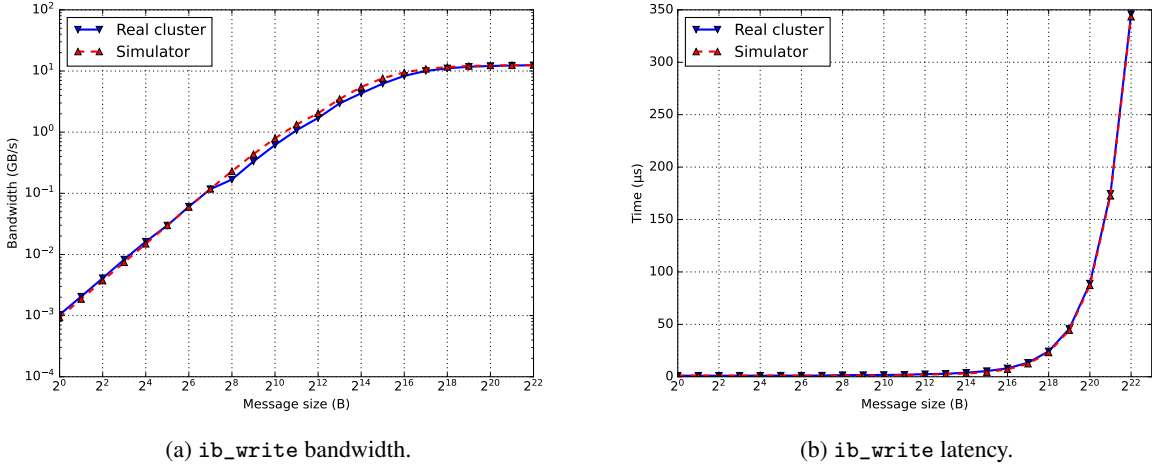


Figure 4: Experiment results in the real cluster and the simulator when communicating two end-node devices.

to the inter-node network. Table 1 shows that maximum bandwidth is achieved with 128KB messages (i.e., the PCIe MPS). For larger messages, latency skyrockets due to this bottleneck, as TLPs accumulate in the intra-node network while waiting to be split into InfiniBand packets.

We modeled the `ib_write` Infiniband test in our simulator to validate the PCIe intra-node model. Figure 4 shows the bandwidth and latency results obtained running the `ib_write` test both in the simulator and the real cluster. Figure 4a compares the bandwidth results, which are virtually identical between the two series. Figure 4b shows the latency results that follow the same trend. These results show that, in this simple scenario, the PCIe intra-node model essentially behaves as expected. It splits conveniently PCIe transactions into TLPs (i.e., intra-node packets) sent through the end-node NIC device, which compose a network packet each with MTU = 4KB. These packets are sent through the InfiniBand network and, when received at the destination NIC, they are transformed again into TLPs and forwarded to the receiving buffer at the host-side user space application, so the performance metrics are measured.

Note that the intra-node network model is fully configurable to behave not only as PCIe but also to be as generic as possible. In the following sections, we extend the analysis to the results of scale-out simulations using generic intra- and inter-node configurations.

4.2 Scale-out simulation experiments

To analyze the impact of intra-node communication involving multiple accelerators per node on large inter-node networks, we have configured the simulation model (see Section 3.3) to operate similarly to those intra- and inter-node networks commonly used in Datacenters and Supercomputers. This section shows the simulation results for large network configurations (see Table 3) when different realistic traffic patterns are used. In the following sections, we describe the experiments' configuration (i.e., the intra- and inter-node network configuration and the communication patterns) and analyze the simulation results.

4.2.1 Intra- and inter-node network configurations

We have modeled the end-node architecture similarly to that of modern compute nodes. We assume each end node includes 8 accelerators interconnected by a high-speed intra-node network. Each accelerator has a NIC to enable data generation in the intra-node network. We assume that the intra-node network can operate at the following aggregated speeds:

- 128 GB/s: Each accelerator NIC has a data rate of 128 Gbps, so the aggregated intra-node network bandwidth among all accelerators is $8 \times 128 = 1024$ Gbps (i.e., 128 GB/s).
- 256 GB/s: Each accelerator NIC data rate is 256 Gbps, the aggregated intra-node network bandwidth being 256 GB/s.
- 512 GB/s: Each accelerator NIC data rate is 512 Gbps, the aggregated intra-node network bandwidth being 512 GB/s.

These link speeds and aggregated bandwidth are consistent with several intra-node network technologies, such as PCIe or Infinity Fabric [18], which use a bandwidth per link similar to the inter-node network link. Unfortunately, the aggregated bandwidth of the intra-node network is much larger than that of a single inter-node network link, so this shows clearly that end-node NICs might be the bottleneck if all the end-node devices would want to communicate at full speed to devices at different end nodes.

Table 3 shows the inter-node network configurations. We have configured 32- and 128-node inter-node networks using a Real-Life Fat-Tree (RLFT) topology [19]. As we assume 8 accelerators per node, the total number of accelerators interconnected using the intra- and inter-node networks is 256 and 1024, respectively.

Table 3: Network configurations used in the experiments.

#	Nodes	Accelerators	Topology	Inter-node switches	Routing
1	32	256	RLFT	12	D-mod-K
2	128	1024	RLFT	24	D-mod-K

We assume 400 Gbps links for the inter-node network, consistent with current high-speed networking technologies such as InfiniBand or Gigabit Ethernet. The latency for the first flit of a packet traversing the inter-node network is set to 6 ns. The switching policy is virtual cut-through, and the flow control mechanism is credit-based. We assume the *D-mod-K* deterministic routing algorithm [20] for both network configurations, which efficiently balances traffic flows paths among available shortest routes.

Regarding the performance metrics, we measured the *intra-node latency* that measures the time required for an intra-node packet to be sent and received within the same end node. It excludes packets that traverse the inter-node network. We also modeled the *intra-node throughput* that measures the average data rate per time unit (in GB/s) transmitted within the intra-node networks. We have also measured the *inter-node throughput* that measures the data rate transmitted through the inter-node network. Finally, we also measure the *Flow Completion Time (FCT)* that measures the total time taken for a message to be transmitted from its generation at the source accelerator until its reception at the destination.

4.2.2 Communication patterns configuration

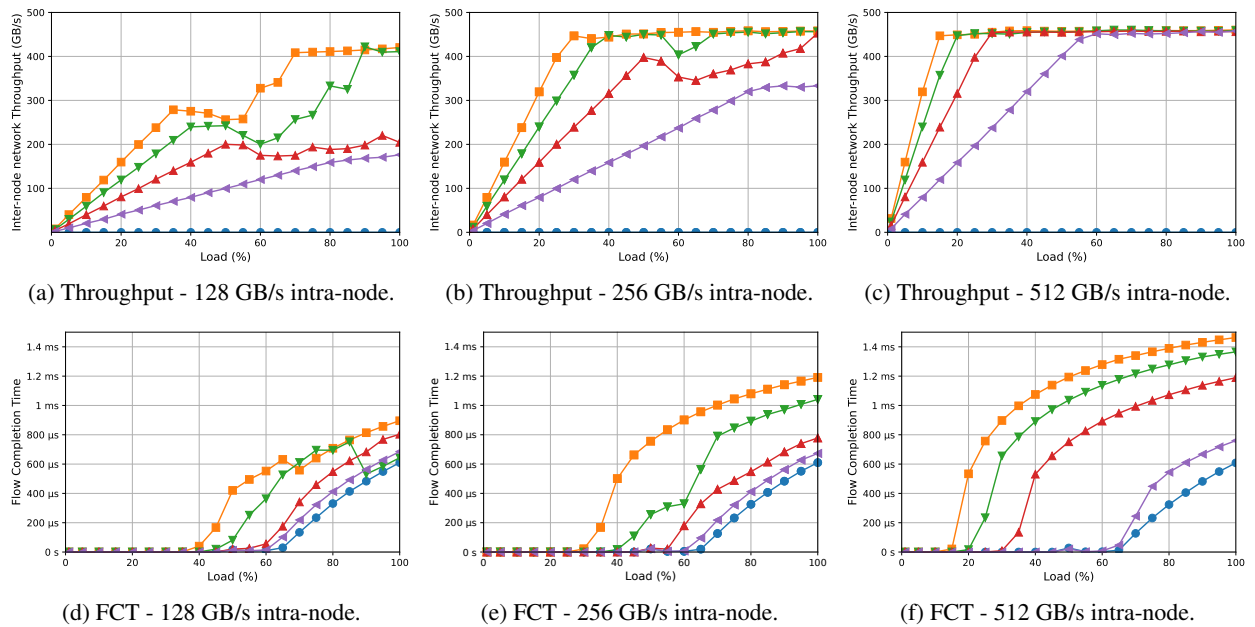
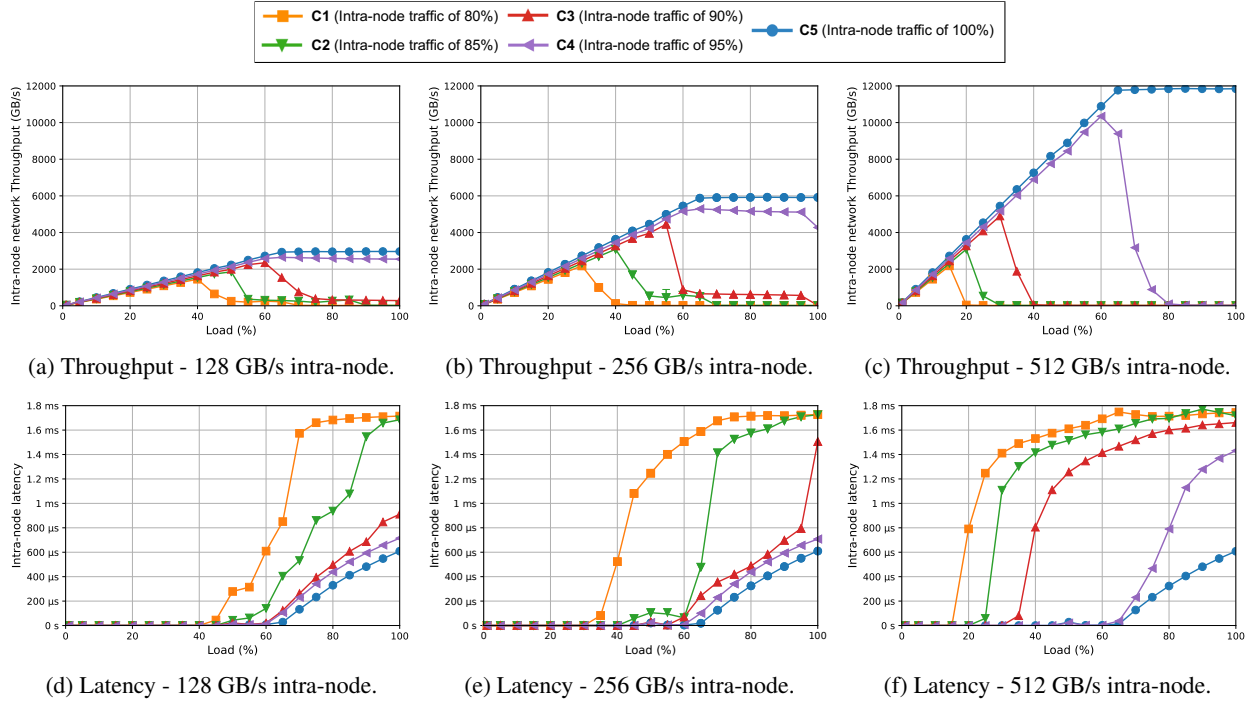
Our experiments have evaluated the impact of intra-node and inter-node communication on system performance. To achieve this, we explore different DP, PP, and PP configurations (see Section 3.4). We have considered five communication patterns: $C1, C2, C3, C4, C5$, which differ on the amount of traffic generated at the accelerators addressed to the intra- and inter-node network. In other words, we vary the amount of messages generated due to data and model parallelism. However, this configuration does not imply that these communication patterns belong to specific LLM models. Note that determining the most efficient and optimal configuration for the different types of parallelism (e.g., DP, PP or TP) for a specific LLM is beyond the scope of our work. For such purposes, existing tools such as Calculon [21] can provide valuable insights.

For all the communication patterns, accelerators generate 4KiB messages to the intra-node network at rates from 0 to 100% of their NIC links capacity (i.e., 128, 256, and 512 Gbps). We simulated 20 traffic load values per traffic pattern, each comprising 2.5ms of simulation time where messages are generated at a specific load. After this time, we measure the performance metrics during 0.5ms. For intra-node traffic, message destinations are chosen randomly among the accelerators within an end node. For inter-node traffic, destinations are selected randomly among all the possible end-node devices distinct from where these messages are generated.

4.2.3 Analysis of simulation results

Figure 5 illustrates the intra- and inter-node performance results versus traffic load for a 32-node RLFT network (i.e., 256 accelerators) when the $C1$ -to- $C5$ traffic patterns are generated into the three different intra-node configurations. Note that inter-node network NICs can handle up to 400 Gbps (i.e., 50 GB/s), while the intra-node network can inject up to 128, 256, or 512 GB/s, depending on the network configuration. As we can see in Figures 5a, 5b and 5c the maximum aggregated intra-node network throughput increases proportionally to the aggregated intra-node bandwidth. The saturation point² in terms of generated intra-node traffic load is reached when more inter-node traffic is generated (e.g., $C1$), and this situation becomes worse as the aggregated intra-node bandwidth increases (see Figure 5c). The same trends as for intra-node throughput can be observed if we look at intra-node latency metrics (see Figures 5d, 5e and 5f).

²Note that the network saturation point is where throughput drops to zero due to NIC buffers collapse and packets are not able to reach the destination during the simulation time, and latency skyrockets.



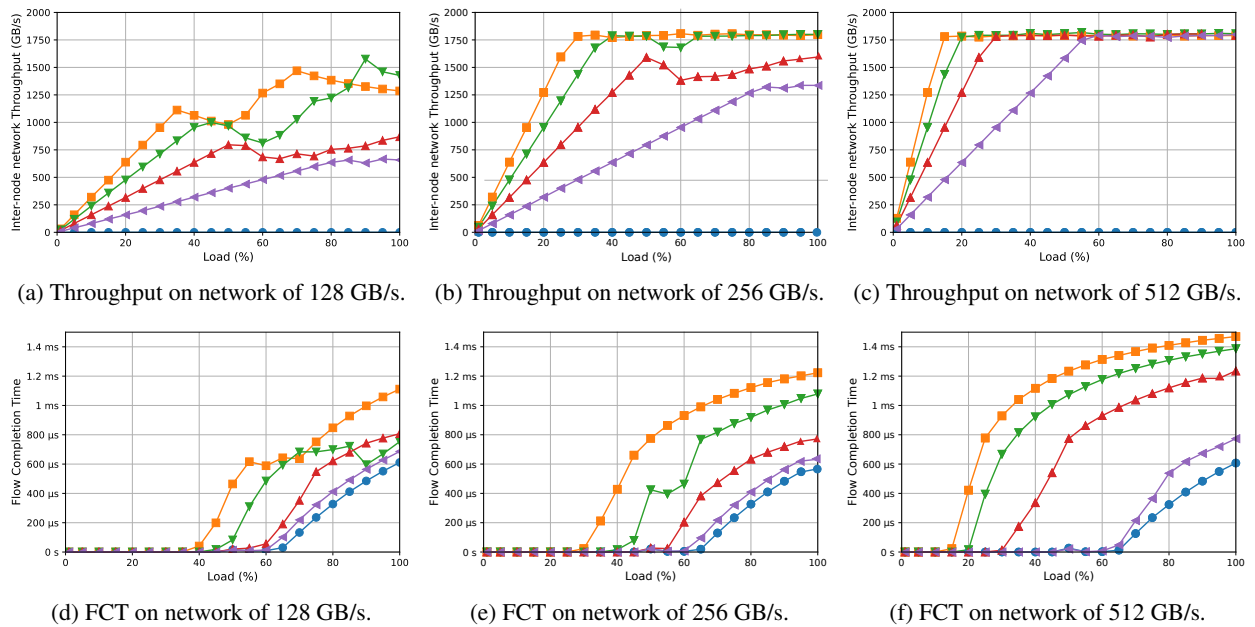
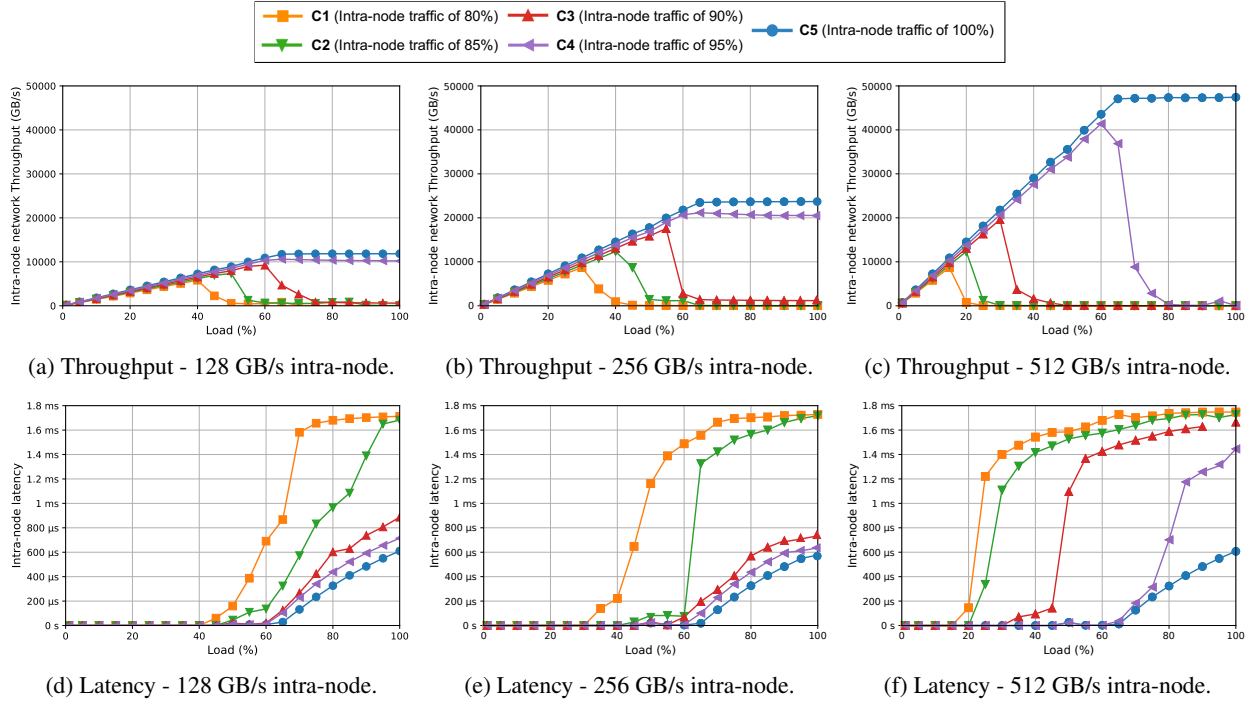


Figure 6 shows the inter-node network throughput and FCT metrics for the same scenarios. As we can see, communication patterns $C1$ and $C2$ achieve the best inter-node throughput even though they saturate soon in the intra-node network. Presumably, this is because these communication patterns generate the largest amount of inter-node traffic. By contrast, as it can be seen in Figures 6d, 6e and 6f, where we can see that communication patterns $C1$ and $C2$ achieve the worst performance due to the intra-node bottleneck described above. Another interesting aspect regarding latencies (intra-node latency and FCT) is that they increase exponentially as the inter-node network injects traffic. This indicates the presence of two distinct bottlenecks: at the source end-node and the destination end-node. At both sides, messages destined for the inter-node network must traverse their respective NICs, which are bottlenecked due to the saturation. The source end-node's NIC is limited to handling a maximum of 50 GB/s. Meanwhile, the destination end-node's NIC packetizes inter-node packets (of 4 KiB) into intra-node packets of 128 B, injecting a large number of packets from the inter-node network into the intra-node network.

Focusing on traffic patterns, as TP increases, leading to greater traffic injection into the inter-node network, the overall system performance degrades due to increased contention at the end-node NICs and the emergence of bottlenecks. This does not necessarily indicate a reduction in LLM computational performance, as multiple accelerators still collaborate to accelerate sub-layer processing. However, it is crucial to analyze network impact, as excessive communication delays can degrade overall LLM performance.

Figures 5 and 6 show that increasing intra-node network aggregated bandwidth may negatively affect overall network performance under certain communication patterns (e.g., LLMs with a high degree of TP). Note that increasing intra-node bandwidth enhances performance when traffic remains confined within the intra-node network (as in configuration $C5$), but this differs for other configurations ($C1$, $C2$, $C3$, and $C4$), where the additional traffic injected into the inter-node network spoils intra-node network throughput as intra-node bandwidth increases. Conversely, the inter-node network benefits from this increased intra-node bandwidth, as more traffic can be handled.

Figures 7 and 8 show that increasing the network size to a 128-node RLFT topology (i.e., 1024 accelerators) does not alter the trends observed for the 32-node configuration. For the intra-node network, the throughput and latency trends remain consistent. The throughput scales proportionally with the number of nodes; as there are four times more accelerators in the 128-node topology. However, the intra-node latency remains unchanged because the intra-node network configuration and the number of accelerators per node are identical to those in the smaller topology. Thus, similar observations can be made regarding the inter-node network and FCT. Since the bottleneck originates in the intra-node network, the inter-node network exhibits the same tendencies observed in the smaller topology. Throughput in the inter-node network increases proportionally with the number of nodes, reflecting the higher data exchange between nodes. In summary, these results demonstrate the impact of the intra-node network traffic on the overall system performance. Bottlenecks within the intra-node network have significant downstream effects on the inter-node network, underscoring the importance of optimizing intra-node communication for scaling large systems effectively.

5 Conclusions

This paper has analyzed the impact of the interference between intra- and inter-node communication operations generated by emerging applications (e.g., generative AI or LLMs) in Supercomputers and Datacenters. To help with this research, we have developed a detailed packet-level simulation model validated against a real cluster infrastructure using standard micro-benchmarks, demonstrating its accuracy and reliability. Additionally, we conducted scale-out simulation experiments to model large heterogeneous computing and storage clusters, scaling up to 1024 end-node devices (e.g., accelerators). We have also modeled realistic communication patterns based on LLM programming model using different types of parallelism (data, pipeline and tensor parallelism), which have been used to feed our simulation tool. Our analysis has identified a critical bottleneck at the interface between the intra-node network and the NIC link, which significantly impacts the performance of both intra- and inter-node networks and reduces overall system performance. We have also observed that increasing or decreasing the number of nodes in a supercomputer does not fundamentally alter this bottleneck's impact, as the intra-node network's limitations remain the dominant factor. Our simulation and the findings related to intra- and inter-node communication dynamics provide valuable insights to improve the design of large-scale heterogeneous computing environments.

References

[1] Deepak Narayanan, Mohammad Shoeybi, Jared Casper, Patrick LeGresley, Mostofa Patwary, Vijay Anand Korthikanti, Dmitri Vainbrand, Prethvi Kashinkunti, Julie Bernauer, Bryan Catanzaro, Amar Phanishayee, and Matei Zaharia. Efficient Large-Scale Language Model Training on GPU Clusters Using Megatron-LM, August 2021. arXiv:2104.04473 [cs].

- [2] Daniele De Sensi, Lorenzo Pichetti, Flavio Vella, Tiziano De Matteis, Zebin Ren, Luigi Fusco, Matteo Turisini, Daniele Cesarini, Kurt Lust, Animesh Trivedi, Duncan Roweth, Filippo Spiga, Salvatore Di Girolamo, and Torsten Hoefer. Exploring gpu-to-gpu communication: Insights into supercomputer interconnects. In *SC24: International Conference for High Performance Computing, Networking, Storage and Analysis*, pages 1–15, 2024.
- [3] Nathan Binkert, Bradford Beckmann, Gabriel Black, Steven K. Reinhardt, Ali Saidi, Arkaprava Basu, Joel Hestness, Derek R. Hower, Tushar Krishna, Somayeh Sardashti, Rathijit Sen, Korey Sewell, Muhammad Shoaib, Nilay Vaish, Mark D. Hill, and David A. Wood. The gem5 simulator. *SIGARCH Comput. Archit. News*, 39(2):1–7, aug 2011.
- [4] Saptarshi Bhowmik, Nikhil Jain, Xin Yuan, and Abhinav Bhatele. A simulation study of hardware parameters for future gpu-based hpc platforms. In *2021 IEEE International Performance, Computing, and Communications Conference (IPCCC)*, pages 1–10, 2021.
- [5] Nikhil Jain, Abhinav Bhatele, Sam White, Todd Gamblin, and Laxmikant V. Kale. Evaluating hpc networks via simulation of parallel workloads. In *Proceedings of the International Conference for High Performance Computing, Networking, Storage and Analysis, SC '16*. IEEE Press, 2016.
- [6] NVIDIA H100 Tensor Core GPU Architecture Overview, December 2024. [Online; accessed 18. Dec. 2024].
- [7] NVIDIA Grace Hopper Superchip Architecture Whitepaper, December 2024. [Online; accessed 18. Dec. 2024].
- [8] Intel® Gaudi® 3 AI Accelerator White Paper, December 2024. [Online; accessed 18. Dec. 2024].
- [9] Torsten Hoefer, Ariel Hendel, and Duncan Roweth. The convergence of hyperscale data center and high-performance computing networks. *Computer*, 55(7):29–37, 2022.
- [10] Andrea Biagioni and et al. Red-sea: Network solution for exascale architectures. In *2022 25th Euromicro Conference on Digital System Design (DSD)*, pages 712–719, 2022.
- [11] Shekhar Borkar and Andrew A. Chien. The future of microprocessors. *Communications of the ACM*, 62(5):44–52, 2019.
- [12] Christopher J Shallue, Jaehoon Lee, Joseph Antognini, Jascha Sohl-Dickstein, Roy Frostig, and George E Dahl. Measuring the effects of data parallelism on neural network training. *arXiv preprint arXiv:1811.03600*, 2018.
- [13] Mohammad Shoeybi, Mostofa Patwary, Raul Puri, Patrick LeGresley, Jared Casper, and Bryan Catanzaro. Megatron-lm: Training multi-billion parameter language models using model parallelism. *arXiv preprint:1909.08053*, 2019.
- [14] Yanping Huang, Orhan Firat, HyoukJoong Lee, Yonghui Wu, Youlong Cheng, Mia XuChen, Jiquan Ngiam, Ankur Bapna, Dehao Chen, Quoc V Le, and Zhifeng Chen. Gpipe: Easy scaling with micro-batch pipeline parallelism. *arXiv preprint arXiv:1811.06965*, 2019.
- [15] Pedro Yébenes, Jesus Escudero-Sahuquillo, Pedro J. García, Francisco J. Alfaro, and Francisco J. Quiles. Providing differentiated services, congestion management, and deadlock freedom in dragonfly networks. In *2016 2nd IEEE International Workshop on High-Performance Interconnection Networks in the Exascale and Big-Data Era (HiPINEB)*, pages 33–40, 2016.
- [16] University Ohio. MVAPICH::Benchmarks, March 2024. [Online; accessed 8. Mar. 2024].
- [17] NVIDIA. Perftest Package, March 2023. [Online; accessed 11. Mar. 2024].
- [18] Gabin Schieffer, Ruimin Shi, Stefano Markidis, Andreas Herten, Jennifer Faj, and Ivy Peng. Understanding data movement in amd multi-gpu systems with infinity fabric, 2024.
- [19] Hridoy Jyoti Mahanta, Abhijit Biswas, and Anwar Hussain. An architecture based routing for heterogeneous fat tree network on chip. In *2015 International Symposium on Advanced Computing and Communication (ISACC)*, pages 341–345, 2015.
- [20] Eitan Zahavi. Fat-tree routing and node ordering providing contention free traffic for mpi global collectives. *Journal of Parallel and Distributed Computing*, 72(11):1423–1432, 2012. Communication Architectures for Scalable Systems.
- [21] Mikhail Isaev, Nic McDonald, Larry Dennison, and Richard Vuduc. Calculon: a methodology and tool for high-level co-design of systems and large language models. In *ACM Conferences*, pages 1–14. Association for Computing Machinery, New York, NY, USA, November 2023.